

## Extended x-ray-absorption fine-structure studies of diamond and graphite

G. Comelli, J. Stöhr, and W. Jark

*IBM Almaden Research Center, San Jose, California 95120-6099*

B. B. Pate

*Stanford Synchrotron Radiation Laboratory, Stanford Linear Accelerator Center, Stanford University, P.O. Box 4349, Stanford, California 94305*

(Received 17 September 1987)

We have recorded the extended x-ray-absorption fine structure (EXAFS) above the carbon *K* edge for diamond and highly oriented crystalline graphite using 250–800-eV synchrotron radiation. The spectra are used to test phase and amplitude transferability of the C—C EXAFS signal between the two bonding forms of carbon. We find excellent phaseshift transferability with errors in distances less than 0.01 Å. Amplitude transferability is worse but better than 20%. Implications of our results for structural determinations of C—C bonds in molecules and solids are discussed.

### I. INTRODUCTION

The extended x-ray-absorption fine-structure (EXAFS) technique has been known and widely used for many years for determining the local structure around specific atomic species.<sup>1</sup> Until now, however, most EXAFS experiments have been carried out on samples in which either or both the absorbing and backscattering atoms were of intermediate- or high-atomic-number *Z*. This is due to the fact that the soft x-rays region, which contains the *K* edges of low-*Z* absorbers such as carbon, nitrogen, and oxygen, has historically been plagued with experimental problems,<sup>2</sup> and that the backscattering amplitude for low-*Z* elements rapidly decays above the absorption edge such that the EXAFS oscillations are less pronounced than for high-*Z* backscatterers. In addition, bonds involving low-*Z* atoms are shorter and therefore fewer EXAFS oscillations are observed.

From a theoretical point of view there are some interesting questions associated with the EXAFS signal from low-*Z* atoms. The fundamental phase<sup>3</sup> and amplitude transferability concepts which underlie modern EXAFS analysis have their theoretical justification in the assumption that the photoelectron scattering process is dominated by the *core* electrons of the absorbing and/or the backscattering atoms. For low-*Z* atoms the total electron density is low, and the valence electrons are a large fraction of the total number of electrons. Hence one might expect the largest valence electron effects on the scattering potentials for low-*Z* atoms resulting in a possible breakdown of the simple EXAFS theory. Other questions regard the observability and practical usability of EXAFS for samples where both the absorbing and backscattering atoms are of low-atomic number. This is clearly the most difficult case to be studied by EXAFS. First, for low-*Z* backscatterers, the decreasing EXAFS amplitude above the edge limits the usable data range and, secondly, the short bond lengths between low-*Z* atoms minimize the number of observable EXAFS wiggles. In order to address the above-mentioned problems

and because of the singular importance of carbon in fields like chemistry and surface science, we present here EXAFS studies of the C—C bonding in the two fundamental forms of carbon, diamond and graphite.

The EXAFS of crystalline and amorphous graphite has been recorded and analyzed before using electron energy loss spectroscopy (EELS) up to 250 eV above the C *K* edge<sup>4–6</sup> or x-ray absorption data up to 170 eV above the edge.<sup>7</sup> For diamond, EXAFS data have also been obtained up to 110 eV above the edge with EELS<sup>6</sup> and up to 250 eV above the edge with x-ray absorption<sup>8</sup> but were not analyzed in detail. The detailed near-edge x-ray-absorption fine structure (NEXAFS) has also been recorded for graphite<sup>9–11</sup> and diamond.<sup>11–13</sup> Besides extending the data range to a photon energy of 800 eV, i.e., > 500 eV above the carbon *K* edge, the present study presents the first analysis of the EXAFS of diamond and compares it in detail to that of graphite.

Our study establishes reliability limits for EXAFS measurements above the C *K* edge. Even for the unfavorable case of C—C bonding studied here EXAFS is found to be a valuable tool. For nearest-neighbor C—C bonds phase-shift transferability is found to work extremely well with error bars of less than 1% for the derived distances, similar as for intermediate and high-*Z* atoms. Amplitude transferability is less reliable. It is found to be better than 20% which is slightly worse than the 15% value typically found for higher *Z* elements.<sup>14–16</sup> Using the nearest-neighbor shell EXAFS signal as a reference we have calculated the EXAFS of more distant shells, and we find good agreement between the observed and calculated signal of all neighbor shells within 4 Å of the central atom. For more distant shells multiple scattering effects are found to be important.

### II. EXPERIMENT

The measurements were performed on beam line I-1 at the Stanford Synchrotron Radiation Laboratory. This beam line is equipped with a grasshopper monochroma-

tor (1200 lines/mm holographic grating). The EXAFS spectra were obtained by total-electron-yield (TEY) detection.<sup>17</sup> Our "graphite" sample was a highly oriented pyrolytic material (monochromator graphite) which was cleaved with Scotch tape before insertion into the sample chamber. It was mounted such that the E vector of the x-rays was parallel to the ring planes (i.e., perpendicular to the crystallographic *c* axis). Before the measurements the sample was heated in UHV in order to remove any adsorbates. The natural type IIb diamond crystal (B doped, semiconducting) had a (111) surface orientation. The crystal was polished using standard procedures<sup>18</sup> and was measured without any processing in UHV. The photon energy was calibrated using the positions of two minima (284.7 and 291.0 eV) in the monochromator transmission function. In order to correct for this structure and to eliminate intensity glitches arising from possible instabilities of the storage ring a double-normalization procedure was employed. Intensity glitches were eliminated by dividing the signal from the sample by the simultaneously recorded TEY signal from a gold grid reference monitor. The so-obtained ratio still contains some EXAFS unrelated structures arising from the energy dependence of the gold quantum yield (*N* edges) in the 250–1000 eV range. These are eliminated by dividing the ratio spectrum a second time by the TEY spectrum of a clean Si(111) wafer, also normalized to the gold grid monitor. Si has a structureless response function over the energy range of interest, and its spectrum is recorded with the same detector as used for the sample. This insures optimum cancellation of all non-EXAFS structures.<sup>19</sup>

### III. EXPERIMENTAL RESULTS AND DATA ANALYSIS

#### A. Distance and coordination number of first-neighbor shell

In Fig. 1 we show the TEY spectra of diamond and graphite, together with the EXAFS signal obtained after background subtraction. The good signal-to-noise ratio of the data allowed us to measure the EXAFS extending to about 500 eV above the edge. In order to check the validity of the phase and amplitude transferability technique, we used graphite as the "standard" model and diamond as the "unknown" system. We first extracted the C—C phase shift and amplitude from the first Fourier transform peak of the graphite data, corresponding to three carbon nearest neighbors (NN) at the known C—C distance of 1.421 Å.<sup>20</sup> We then used the so-determined phase and amplitude functions to determine the C—C distance and coordination number for the first NN shell in diamond.

The EXAFS signal is given by the familiar single-scattering formula

$$\chi(k) = - \sum_i \frac{N_i^*}{kR_i^2} F_i(k) e^{-2\sigma_i^2 k^2} e^{-2R_i/\lambda(k)} \times \sin[2kR_i + \phi_i(k)], \quad (1)$$

where the summation extends over all neighbor shells *i* separated from the absorbing atom by a distance *R<sub>i</sub>* and

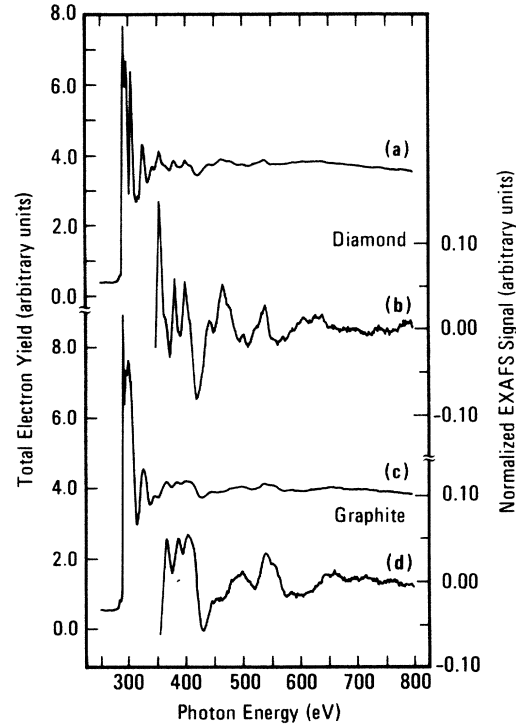


FIG. 1. Total-electron-yield spectra [(a) and (c)] and background-subtracted EXAFS signals [(b) and (d)] for single-crystal diamond and highly oriented pyrolytic graphite. The data were taken at 300 K. For graphite the E vector was parallel to the basal plane such that only the EXAFS from in-plane distances is observed.

effective coordination number  $N_i^*$  given by

$$N_i^* = 3 \sum_{j=1}^{N_i} \cos^2 \alpha_{ij}, \quad (2)$$

where  $\alpha_{ij}$  is the angle between the E vector and the vector  $r_{ij}$  from the central atom to the *j*th atom in the *i*th shell. For our experimental graphite geometry  $N_i^* = 1.5N_i = 4.5$  and for diamond  $N_i^* = N_i = 4$ , independent of crystal orientation.<sup>21</sup>  $\phi_i$  is the phase shift which the photoelectron wave experiences from the absorbing and scattering atoms,  $F_i(k)$  is the backscattering amplitude of the neighbor atoms, and the exponential terms are, respectively, the Debye-Waller-like term and the damping term due to inelastic scattering [mean free path  $\lambda(k)$ ] of the photoelectrons.

The data analysis proceeded along well-established steps, extraction of the EXAFS signal from the normalized TEY spectrum by subtracting a spline polynomial, normalization of the signal to the edge jump,<sup>17</sup> and finally conversion of energy to wave-vector scale. As the energy "zero" we chose the absorption edge of the graphite spectrum  $E_0 = 284$  eV. We then calculated the Fourier transform  $F(r)$  of the graphite EXAFS signal  $\chi(k)k^2$  over the range  $4.5 \leq k \leq 11 \text{ \AA}^{-1}$ , as shown in Fig. 2, and used a window function to minimize the effects due to data truncation. In order to isolate the contribution to  $\chi(k)$  of the first shell, we transformed the first peak in  $|F(r)|$  back

into  $k$  space. Using the first shell of graphite we found  $\phi^{C-C}(k)$  to be approximately a linear function of  $k$  in the range investigated. The derived experimental C—C phase shift together with the linear fit

$$\phi^{C-C} = 4.26 - 0.400k \quad (3)$$

are shown in Fig. 3, and they are compared with an *ab initio* calculated curve<sup>22</sup> that can be written in parameterized form as

$$\phi^{C-C} = -2.618 - 1.333k + 0.0475k^2. \quad (4)$$

There is a substantial disagreement between the experimental and the theoretical phase shifts. This is surprising since in the case of another low- $Z$  element, oxygen, the experimental phase shift derived from the O—O distance in ice (2.76 Å) has been found to agree very well with the

theoretical one.<sup>23</sup> A possible explanation is that the bond lengths involved in our case are much shorter (1.4–1.5 Å). This makes more questionable one of the approximations used for the calculation of the theoretical phase shift, namely the use of plane rather than of spherical waves. A similar disagreement between theoretical and experimental phase shifts for low- $Z$  molecules has also been reported by Yang, Kirz, and Sham<sup>24</sup> although their experimental results have been questioned by Hitchcock and Ishii.<sup>25</sup> We have analyzed the graphite data using the theoretical phase shift in order to estimate the error that it causes in the determination of the bond length. As usual in the EXAFS analysis,<sup>26</sup> we introduced an “inner potential”  $\Delta$ (eV) such that the true-energy value for which the photoelectron has zero momentum is given by  $h\nu = E_0 + \Delta$ .  $\Delta$  is treated as an adjustable parameter, compensating for the arbitrary choice of  $E_0$ . The result

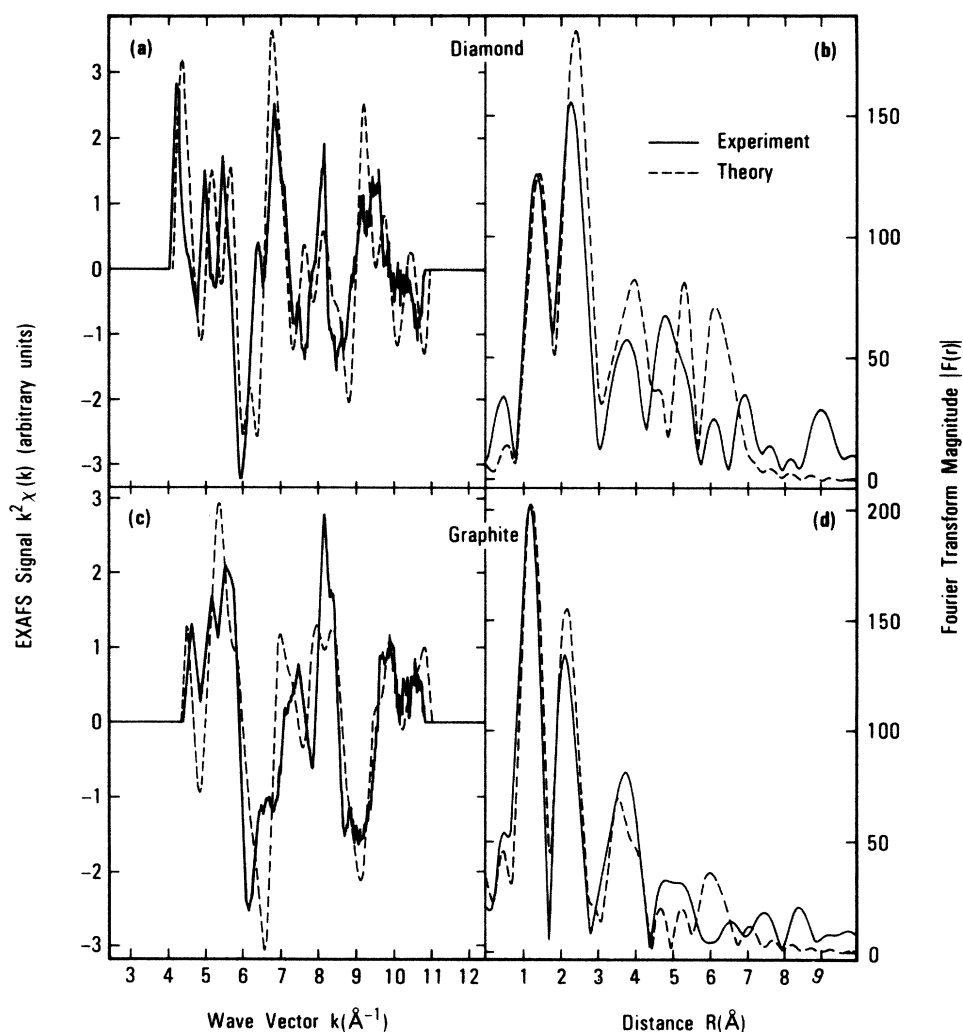


FIG. 2. Comparison between experimental EXAFS signal (solid curves) and single-scattering simulations (dashed curves) for diamond (a) and graphite (b). The simulations were calculated according to Eq. (1) neglecting the exponential terms with use of the phase shift given by Eq. (3) and the amplitude function given by Eq. (6). All neighbor shells listed in Table I were included. The calculated EXAFS signal was scaled by eye to best match the overall size of the experimental oscillations. For graphite the calculated signal was multiplied by a factor 0.6, for diamond by 0.67. (b) and (d) The magnitudes of the Fourier transforms of the data shown in (a) and (c), respectively. The calculated transforms were scaled to the height of the first peak in the experimental transforms.

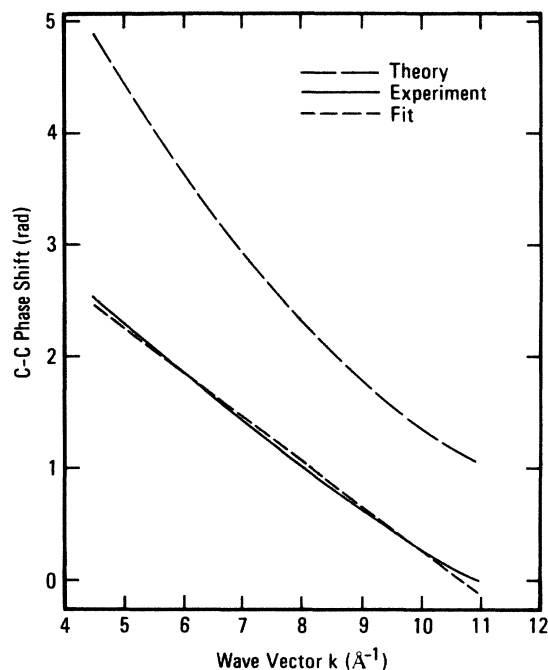


FIG. 3. Comparison between the theoretical C—C phase shift calculated by Teo and Lee (Ref. 22) and that derived from the C—C nearest-neighbor distance in graphite. A fit of the experimental phase shift to a linear function (see text) is also shown.

for the C—C distance in graphite was 1.43 Å, still in good agreement with the known value 1.421 Å, but it was necessary to use a very large value of  $\Delta=39$  eV. This is in qualitative agreement with the results of Denley *et al.*<sup>7</sup> who also had to use an unusually large value of  $\Delta=24$  eV in their early EXAFS work on graphite.

We then used the experimental graphite phase shift to determine the C—C distance in diamond. We analyzed the diamond data with the same procedure and parameters used for graphite. In our case, the best result was obtained with  $\Delta=-2$  eV. The distance obtained for the C—C first-neighbor distance in diamond was  $1.54\pm 0.01$  Å, in excellent agreement with the known distance of 1.544 Å.<sup>20</sup> This demonstrates the applicability of the phase-shift-transferability concept even for a low-Z element in two different chemical bonding configurations.

Another aspect of our investigation is the question of amplitude transferability in order to obtain coordination numbers and Debye-Waller factors. The amplitudes  $|X_{1G}(k)|$  and  $|X_{1D}(k)|$  corresponding to the first-shell signals of graphite and diamond, respectively, are linked by the equation

$$\ln \frac{|X_{1G}(k)|}{|X_{1D}(k)|} = \ln \frac{N_{1G}^* R_{1D}^2}{N_{1D}^* R_{1G}^2} + 2k^2(\sigma_{1D}^2 - \sigma_{1G}^2) \quad (5)$$

provided that the backscattering amplitude  $F(k)$  is the same for diamond and graphite. Plotting the natural logarithm of the ratio versus  $k^2$  one can determine the difference of the Debye-Waller factors from the slope,

and the ratio of the coordination numbers from the intercept at  $k^2=0$ . Using graphite with  $N_{1G}^*=4.5$  as our model we can use Eq. (5) to determine  $N_{1D}^*$  for diamond and compare it to the known value  $N_{1D}^*=4$ . It is clear that care has to be exercised in analyzing EXAFS data involving low-Z absorbers and backscatters. Since the bond lengths involved are very short, only few EXAFS oscillations are observed. Moreover, the C—C backscattering amplitude is very weak and drops rapidly with increasing  $k$ .<sup>22</sup> In order to check the dependence of the results on the analysis procedure we analyzed the graphite and diamond data in different ways, involving variations in background subtraction procedures and use of different window functions both in wave vector and distance space. We found that the amplitude ratio was indeed sensitive to the analysis procedure. Using the same procedures for the analysis of both the graphite and diamond data the NN coordination number in diamond could be predicted to better than 20% using graphite as a model. It is interesting to note that the diamond coordination number was always determined to be too small. The reliable determination of the coordination number of diamond may be impeded not by limitations of the amplitude-transferability concept, but rather, by the fact that the total measured EXAFS signal is dominated by higher shell contributions. In fact, it is hard to directly see the first-shell oscillations in the measured signal. Because of the limited data range used in the EXAFS analysis the presence of strong signals from higher shells will have an effect on the first-shell signal even if the different shell contributions are separated in the transform. In this light and the 15% coordination number accuracies typically quoted for intermediate- and high-Z atoms<sup>16</sup> our results are not surprising. In fact, they show that EXAFS can also serve as a valuable structural technique for the investigation of bonds between low-Z atoms.

#### B. Analysis of higher-neighbor shells

In order to investigate whether the peaks beyond the first in the Fourier transforms shown in Fig. 2 may be explained by the simple single-scattering picture, we generated theoretical spectra for diamond and graphite using Eq. (1). For  $F(k)$  of carbon we used the theoretical amplitude curve proposed by Teo and co-workers,<sup>27</sup> which in parametrized form is given by

$$F(k) = \frac{2.122}{1 + 0.3999(k - 0.876)^2} \quad (6)$$

For  $\phi^{C-C}$  we used the experimental phase shift given by Eq. (3). The summation in Eq. (1) was extended over all atoms within about 7 Å of the absorber listed in Table I. In our simulation we neglected the exponential terms in Eq. (1). The Debye-Waller-like term is expected to be relatively unimportant, since the mean-square amplitudes of vibration are very small (about 0.003 Å<sup>2</sup>) for both diamond and in-plane motions in graphite.<sup>20,28</sup> Arguments for neglecting the damping term related to the mean free path  $\lambda(k)$  will be presented below. Experimental and calculated EXAFS signals and their respective Fourier transforms are compared in Fig. 2 for both graphite and

TABLE I. Parameters for neighbor shells of atoms in diamond and graphite.

Neighbor $j$	Occupancy of shell $N_j$	Quality <sup>a</sup> factor $Q$	Distance $R_j$ (Å)
Diamond			
1	4	4.00	1.544
2	12	4.50	2.521
3	12	3.27	2.956
4	6	1.12	3.566
5	12	1.90	3.883
6	24	3.00	4.368
7	16	1.78	4.636
8	12	1.13	5.042
9	24	2.05	5.278
10	24	1.80	5.634
11	12	0.84	5.848
12	8	0.50	6.176
13	24	1.41	6.362
14	48	2.57	6.668
15	36	1.83	6.847
16	6	0.28	7.132
Graphite			
<sup>b</sup> 1	3	3.0	1.421
2	6	2.0	2.461
3	3	0.75	2.842
4	6	0.86	3.759
5	6	0.66	4.263
6	6	0.50	4.922
7	6	0.46	5.123
8	3	0.19	5.684
9	6	0.31	6.193
10	12	0.57	6.512
11	3	0.12	7.105

<sup>a</sup>The quality factor is defined as  $Q = N_j(R_1/R_j)^2$ .

<sup>b</sup>Only in-plane distances are listed.

diamond. All spectra were analyzed in the same way. The agreement is quite good in the light of the simplicity of the model. All peaks up to 7 Å in the Fourier transforms of the original data are also present in the simulations. Especially for graphite, all neighbor shells within 4.5 Å are well accounted for in terms of the positions and relative height of the peaks. In diamond the agreement for the shells within 4.5 Å is also good in terms of peak positions but less good in terms of peak heights. Above 4.5 Å there are considerable discrepancies. This is attributed to stronger multiple scattering effects in diamond than in graphite. The higher atomic density in diamond results in a larger number of multiple scattering paths which are ignored in our single-scattering analysis.

We still have to substantiate the decision of neglecting the damping term due to inelastic scattering in our simulations. Inspection of Figs. 2(b) and 2(d) shows that the neglect of the exponential terms leads to an overestimation of the contribution of the higher shells in diamond.

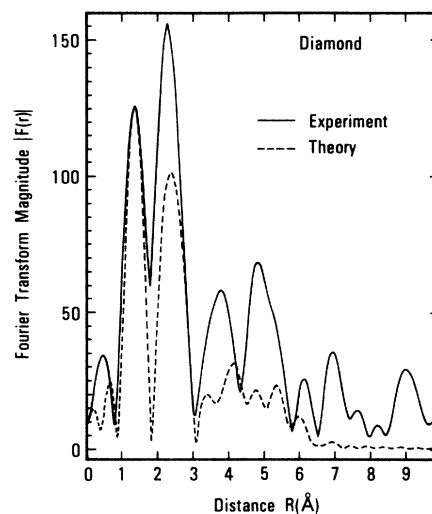


FIG. 4. Comparison between the Fourier transform magnitudes of the diamond EXAFS data [Fig. 2(a)] and of a model that takes into account the exponential damping term due to inelastic scattering as discussed in the text.

In contrast, Fig. 4 shows a simulation where the mean free path term in Eq. (1) has been taken into account. Here, we have used for the electron mean free path  $\lambda(k)$  a fit<sup>29</sup> to the universal curve,<sup>30</sup>

$$\lambda(y) = 43.19 - 22.745y - 5.8044y^2 + 3.6208y^3, \quad (7)$$

where  $y$  is the  $\log_{10}$  of the electron kinetic energy. Figure 4 shows that inclusion of the damping term substantially underestimates the contributions from higher shells and that the differences are larger than when the term is omitted. An analogous result was obtained for graphite. We conclude that  $\lambda(k)$  is on average larger than expected from the universal curve in the electron kinetic energy range 60–500 eV. A quantitative estimate of this effect is beyond the scope of this paper. It is of interest to note, however, that for diamond Pate *et al.*<sup>31</sup> have also found larger values for  $\lambda(k)$  in the 55–115 eV kinetic energy range than the ones predicted by Eq. (7).

Finally a comment is needed regarding the  $k$  range of the data used in the graphite EXAFS analysis. Initially we used a data range 3.2–11 Å<sup>-1</sup>, but the Fourier transform showed a peak between the first- and second-neighbor peak that could not be related to any real distance in graphite. In order to investigate this aspect, we analyzed the data several times, changing the parameters of the analysis, i.e., the width of the window function, the power of  $k$  used to enhance the high- $k$  region, and the  $k$  range. It was found that the data in the  $k$  range below  $k = 4.5$  Å<sup>-1</sup> were indeed responsible for this spurious peak. The reason for this is evident from Fig. 5, where we show a comparison between EXAFS theory and experiment. It is clear that the agreement here is much worse, and that the two signals are completely out of

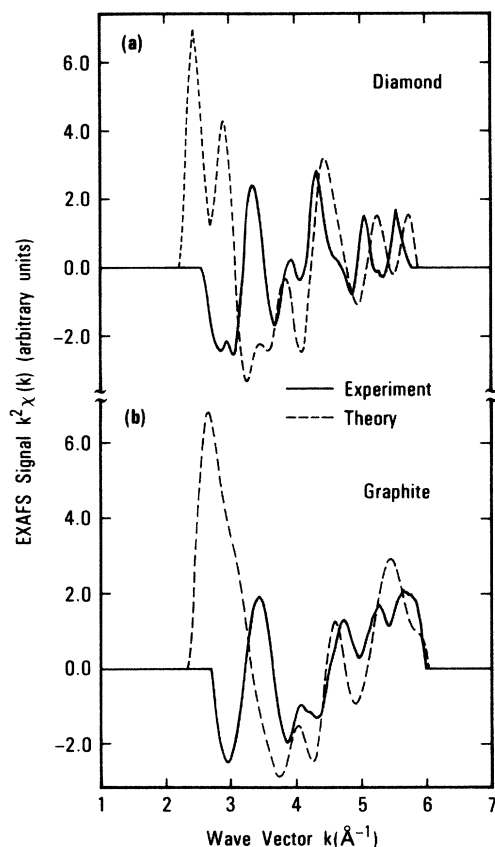


FIG. 5. Comparison between the experimental EXAFS signal and single-scattering simulations in the low- $k$  region for diamond (a) and graphite (b). Calculations were carried out as for Fig. 2.

phase. Thus the signal at low  $k$ , which appears with a new frequency, gives rise to the spurious Fourier transform peak. There are two possible explanations for the effect shown in Fig. 5. First, the C—C phase shift could exhibit a strong nonlinearity below  $k=4.5 \text{ \AA}^{-1}$  due to the larger influence of the valence electron potential at low  $k$  or the breakdown of the small-atom approximation.<sup>32</sup> Secondly, the signal at low  $k$  may simply be dominated by multiple scattering effects involving higher shells. This is favored by the small mean-square displacement of the in-plane carbon atoms and the longer electron mean free paths at low  $k$ . In addition, as pointed out by Bunker and Stern<sup>33</sup> multiple scattering effects are expected to be important in the near-edge region when the bond lengths involved are smaller than  $1.6 \text{ \AA}$  and there is no inversion symmetry, as in graphite and diamond.

#### IV. CONCLUSIONS

We have shown that, in general, EXAFS investigations of C—C bonds are not only possible but can be expected to provide bond lengths of about 1% and first-NN coordination numbers of 20% accuracy. These conclusions are derived from a comparative analysis of the EXAFS of graphite and diamond. We found that in the energy region above the edge corresponding to a wave vector larger than  $4.5 \text{ \AA}^{-1}$  the data could be interpreted for all but the more distant neighbor shells by using the standard single-scattering EXAFS equation. In particular, we showed that the phase-shift-transferability concept can be extended to bonds between low- $Z$  atoms. Amplitude transferability was found to be less reliable, but the errors made in the determination of coordination numbers were not very different than those encountered in previous EXAFS measurements on higher  $Z$  atoms. The mean free path of electrons in diamond was found to be on average longer than predicted by the universal curve. We also pointed out that the region below  $4.5 \text{ \AA}^{-1}$  cannot be explained by extrapolation of the single-scattering EXAFS analysis used for the high- $k$  region.

Our study of the two standard  $sp^2$  and  $sp^3$  configurations of carbon existing in nature is hoped to lay the foundation for the structural investigation of more complex carbonaceous systems. For example, amorphous carbon films are known to exhibit very different physical properties depending on preparation procedures,<sup>34</sup> but the microscopic structure still remains a puzzle. Also, although surface EXAFS or SEXAFS studies of chemisorbed hydrocarbons have recently been reported<sup>35</sup> the determination of intramolecular C—C bond lengths has not been achieved. Our study provides the C—C phase shift needed for the determination of distances in such systems and points out boundary conditions for the determination of coordination numbers.

#### ACKNOWLEDGMENTS

We would like to thank D. A. Outka for implementing the EXAFS analysis software used here and P. Stevens and J. Solomon for help with the measurements. We would like to thank Dr. F. A. Raal of the DeBeers Diamond Research Laboratory (Johannesburg, South Africa) for providing the natural diamond crystal. B. B. Pate acknowledges support from the U.S. Office of Naval Research, Grant No. N00014-87-K-0262. This work was carried out at the Stanford Synchrotron Radiation Laboratory, which is supported by the Office of Basic Energy Sciences of U.S. Department of Energy (DOE) and the Division of Materials Research of the National Science Foundation (NSF).

<sup>1</sup>For reviews of EXAFS spectroscopy, see (a) *EXAFS Spectroscopy, Techniques, and Applications*, edited by B. K. Teo and D. C. Joy (Plenum, New York, 1981); (b) P. A. Lee, P. H. Citrin, P. Eisenberger, and B. M. Kincaid, *Rev. Mod. Phys.* **53**, 769 (1981); (c) *Principles, Applications, Techniques of EXAFS*,

*SEXAFS, and XANES*, edited by D. C. Koningsberger and R. Prins (Wiley, New York, 1988).

<sup>2</sup>J. Stöhr, R. Jaeger, J. Feldhaus, S. Brennan, D. Norman, and G. Apai, *Appl. Opt.* **19**, 3911 (1980).

<sup>3</sup>P. H. Citrin, P. Eisenberger, and B. M. Kincaid, *Phys. Rev.*

- Lett. **36**, 1346 (1976).
- <sup>4</sup>B. M. Kincaid, A. E. Meixner, and P. M. Platzman, Phys. Rev. Lett. **40**, 1296 (1978).
- <sup>5</sup>M. M. Disko, O. L. Krivanek, and P. Rez, Phys. Rev. B **25**, 4252 (1982).
- <sup>6</sup>J. Fink, T. Müller-Heinzerling, J. Pflüger, A. Bubenzer, P. Koidl, and G. Crecelius, Solid State Commun. **47**, 687 (1983).
- <sup>7</sup>D. Denley, P. Perfetti, R. S. Williams, D. A. Shirley, and J. Stöhr, Phys. Rev. B **21**, 2267 (1980).
- <sup>8</sup>B. B. Pate, Ph.D. thesis, Stanford University, 1986.
- <sup>9</sup>R. F. Egerton and M. J. Whelan, J. Electron Spectrosc. Relat. Phenom. **3**, 232 (1974).
- <sup>10</sup>R. A. Rosenberg, P. J. Love, and V. Rehn, Phys. Rev. B **33**, 4034 (1986).
- <sup>11</sup>J. F. Morar, F. J. Himpsel, G. Hollinger, J. L. Jordan, G. Hughes, and F. R. McFeely, Phys. Rev. B **33**, 1346 (1986).
- <sup>12</sup>R. F. Egerton and M. J. Whelan, Philos. Mag. **30**, 739 (1974).
- <sup>13</sup>J. F. Morar, F. J. Himpsel, G. Hollinger, G. Hughes, and J. L. Jordan, Phys. Rev. Lett. **54**, 1960 (1985).
- <sup>14</sup>E. A. Stern, B. A. Bunker, and S. M. Heald, Phys. Rev. B **21**, 5521 (1980).
- <sup>15</sup>B. Lengeler and P. Eisenberger, Phys. Rev. B **21**, 4507 (1980).
- <sup>16</sup>P. Eisenberger and B. Lengeler, Phys. Rev. B **22**, 3551 (1980).
- <sup>17</sup>J. Stöhr, C. Noguera, and T. Kendelewicz, Phys. Rev. B **30**, 5571 (1984).
- <sup>18</sup>B. B. Pate, Surf. Sci. **165**, 83 (1986).
- <sup>19</sup>D. A. Outka and J. Stöhr, J. Chem. Phys. (to be published).
- <sup>20</sup>*International Tables for X-ray Crystallography*, edited by N. F. M. Henry and K. Lonsdale (Kynoch, Birmingham, 1969).
- <sup>21</sup>J. Stöhr, R. Jaeger, and S. Brennan, Surf. Sci. **117**, 503 (1982).
- <sup>22</sup>B. K. Teo and P. A. Lee, J. Am. Chem. Soc. **101**, 2815 (1978).
- <sup>23</sup>R. A. Rosenberg, P. R. LaRoe, V. Rehn, J. Stöhr, R. Jaeger, and C. C. Park, Phys. Rev. B **28**, 3026 (1983).
- <sup>24</sup>B. X. Yang, J. Kirz, and T. K. Sham, Phys. Lett. **110A**, 301 (1985).
- <sup>25</sup>A. P. Hitchcock and I. Ishii, J. Phys. (Paris) Colloq. **8**, C8-199 (1986).
- <sup>26</sup>P. A. Lee and G. Beni, Phys. Rev. B **15**, 2862 (1977).
- <sup>27</sup>B. K. Teo, P. A. Lee, A. L. Simons, P. Eisenberger, and B. M. Kincaid, J. Am. Chem. Soc. **99**, 3856 (1977).
- <sup>28</sup>R. Chen and P. Trucano, Acta Cryst. A **34**, 979 (1978).
- <sup>29</sup>D. Denley, R. S. Williams, P. Perfetti, D. A. Shirley, and J. Stöhr, Phys. Rev. B **19**, 1762 (1979).
- <sup>30</sup>I. Lindau and W. E. Spicer, J. Electron Spectrosc. Relat. Phenom. **3**, 409 (1974).
- <sup>31</sup>B. B. Pate, M. Oshima, J. A. Silberman, G. Rossi, I. Lindau, and W. E. Spicer, J. Vac. Sci. Technol. A **2**, 957 (1984).
- <sup>32</sup>P. A. Lee and J. B. Pendry, Phys. Rev. B **27**, 95 (1975); E. A. Stern, in *Principles, Applications, Techniques of EXAFS, SEXAFS and XANES*, edited by D. C. Koningsberger and R. Prins (Wiley, New York, 1988).
- <sup>33</sup>G. Bunker and E. A. Stern, Phys. Rev. Lett. **52**, 1990 (1984).
- <sup>34</sup>J. Robertson, Adv. Phys. **35**, 317 (1986).
- <sup>35</sup>D. Arvanitis, K. Baberschke, L. Wenzel, and U. Döbler, Phys. Rev. Lett. **57**, 3175 (1986).